

## Original Investigation | CLINICAL SCIENCES

# Paracentral Acute Middle Maculopathy

## A New Variant of Acute Macular Neuroretinopathy Associated With Retinal Capillary Ischemia

David Sarraf, MD; Ehsan Rahimy, MD; Amani A. Fawzi, MD; Elliott Sohn, MD; Irene Barbazetto, MD; David N. Zacks, MD, PhD; Robert A. Mitra, MD; James M. Klanchnik Jr, MD; Sarah Mrejen, MD; Naomi R. Goldberg, MD, PhD; Robert Beardsley, MD; John A. Sorenson, MD; K. Bailey Freund, MD

**IMPORTANCE** With the advent of more sophisticated imaging systems, such as spectral domain optical coherence tomography (SD-OCT), disruption of the inner segment/outer segment (IS/OS) band, and thinning of the outer nuclear layer (ONL) have been identified in association with acute macular neuroretinopathy (AMN).

**OBJECTIVES** To characterize a new SD-OCT presentation of AMN as a paracentral acute middle maculopathy and to describe multimodal imaging findings that implicate an underlying pathogenesis related to retinal capillary ischemia.

**DESIGN, SETTING, AND PARTICIPANTS** Retrospective observational case series (January 1, 2012, to January 1, 2013) reviewing clinical and imaging data from 9 patients (11 eyes) with AMN at 6 tertiary referral centers. Lesions were classified as type 1 or 2 in relation to the SD-OCT location of the lesion above (type 1) or below (type 2) the outer plexiform layer (OPL) at 6 tertiary referral centers.

**RESULTS** Of the 9 patients, 5 were female and 4 were male (mean age, 47.6 years; range, 21-65 years). All patients presented with an acute paracentral scotoma and demonstrated a classic dark gray paracentral lesion with near-infrared imaging. Visual acuity ranged from 20/15 to 20/30. Six eyes (5 patients) had type 1 SD-OCT lesions, also referred to as paracentral acute middle maculopathy, and 5 eyes (4 patients) had type 2 SD-OCT lesions. Although type 1 lesions lead to inner nuclear layer (INL) thinning, type 2 lesions resulted in ONL thinning. Type 2 lesions were always associated with significant outer macular defects, including disruption of the inner segment/outer segment and outer segment/retinal pigment epithelium bands, whereas type 1 lesions spared the outer macula.

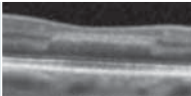
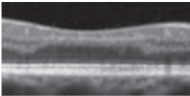
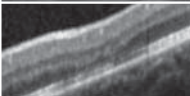
**CONCLUSIONS AND RELEVANCE** Paracentral acute middle maculopathy may represent a novel variant of AMN that affects the middle layers of the macula above the OPL as diagnosed with SD-OCT imaging. Two types of AMN lesions may be seen with SD-OCT occurring above and below the OPL. Type 1 refers to hyperreflective bands in the OPL/INL region with subsequent INL thinning. Type 2 is hyperreflective bands in the OPL/ONL region with subsequent ONL thinning. Type 2 lesions may be associated with concomitant defects of the inner segment/outer segment layer. We propose that each of these lesions may be explained by occlusion of either the superficial capillary plexus (type 1) or deep capillary plexus (type 2) located in the innermost and outermost portion of the INL, respectively, immediately adjacent to each corresponding lesion type.

*JAMA Ophthalmol.* doi:10.1001/jamaophthalmol.2013.4056  
Published online August 8, 2013.

**Author Affiliations:** Author affiliations are listed at the end of this article.

**Corresponding Author:** David Sarraf, MD, Retina Disorders and Ophthalmic Genetics Division, Jules Stein Eye Institute, University of California Los Angeles, 100 Stein Plaza, Los Angeles, CA 90095 (dsarraf@ucla.edu).

Figure 1. Proposed Classification of Acute Macular Neuroretinopathy

	Level of Involvement		Outcome	
Type 1	OPL/INL junction		Atrophy of INL	
Type 2	OPL/ONL junction		Atrophy of ONL	

OPL indicates outer plexiform layer; INL, inner nuclear layer; and ONL, outer nuclear layer.

In the original description of acute macular neuroretinopathy (AMN), Bos and Deutman<sup>1</sup> proposed that the characteristic red, wedge-shaped paracentral lesions of AMN involved the inner layers of the macula. With the advent of more sophisticated imaging systems, such as spectral domain optical coherence tomography (SD-OCT), disruption of the inner segment/outer segment (IS/OS) band was identified in association with AMN, and it was proposed that this disorder be renamed *acute macular outer retinopathy*.<sup>2,3</sup>

More recently, Fawzi et al<sup>4</sup> performed complex multimodal imaging of 8 patients with AMN. Although outer macular lesions, including IS/OS and outer segment/retinal pigment epithelium (OS/RPE) defects and outer nuclear layer (ONL) thinning, developed in most of these eyes, 2 eyes in their series demonstrated more superficial involvement at the levels of the outer plexiform layer (OPL) and the Henle fiber layer (HFL) early in their course. Ischemia of the deep capillary plexus (DCP), located in the outermost portion of the inner nuclear layer (INL), was proposed as the cause of these early OPL lesions.

This report describes 6 eyes (5 patients) with a novel SD-OCT presentation of AMN in which lesions occurred above the OPL in the middle macular region that we have descriptively referred to as a paracentral acute middle maculopathy. We have also included in this study an additional 5 eyes (4 patients) with SD-OCT lesions identified below the OPL, affecting the outer macula and with multimodal imaging evidence of a vasculopathic or ischemic origin. We propose that retinal capillary ischemia affecting either the superficial capillary plexus (SCP) or the DCP may explain the development of either lesion, and we have classified each as either a type 1 (above the OPL) or type 2 (below the OPL) SD-OCT finding.

## Methods

Institutional review board approvals were obtained commensurate with the respective institutional requirements. Research adhered to the tenets of the Declaration of Helsinki and was conducted in accord with regulations set forth by the Health Insurance Portability and Accountability Act.

We retrospectively reviewed the clinical and imaging data from 9 patients (11 eyes) with AMN evaluated at 6 tertiary referral centers, primarily focusing on multimodal imaging correlations. The diagnostic criteria of AMN included a history of acute-onset paracentral scotoma with or without decline in vi-

sual acuity and a nonprogressive course. All patients demonstrated classic paracentral, dark gray, wedgelike lesions with near-infrared (NIR) reflectance and characteristic abnormalities with SD-OCT. We devised a simple classification system to reflect the primary location of SD-OCT lesions in AMN that affected the OPL/INL region of the middle macula (type 1) vs the OPL/ONL region of the outer macula (type 2) (Figure 1).

High-resolution digital color imaging, red-free (RF) photography, and fluorescein angiography (FA) were performed at the time of presentation for each patient. Initial NIR reflectance and SD-OCT examinations (Heidelberg Spectralis HRA+OCT; Heidelberg Engineering) were correlated with subsequent follow-up scans during each patient's follow-up visit. We used the registration feature specific to the Heidelberg Spectralis HRA+OCT, which allows each OCT B scan to be coupled to its exact location on the NIR image, facilitating point-to-point correlations of the retinal findings between the NIR and OCT images.

In addition, patient 9 underwent adaptive optics (AO) imaging using the rtx1 AO retinal camera prototype (Imagine Eyes). The protocol used to capture images with this system has been previously described.<sup>5,6</sup>

## Report of Cases

### Case 1

A 61-year-old white man presented with a 2-week history of a "gray spot" in his right eye just above fixation. He reported significantly higher levels of stress and increased consumption of coffee (10 cups daily compared with his previous amount of 5-7 cups daily) around the time of symptom onset. He denied any recent flulike illness and did not have any relevant medical history.

His best-corrected visual acuity (BCVA) was 20/25 OD and 20/20 OS. Amsler grid testing elucidated a small paracentral scotoma superior to fixation in the affected eye. Ophthalmoscopic examination of the right eye revealed no obvious disease and a normal foveal reflex (Figure 2A). Similarly, the results of FA were unremarkable. However, RF photography revealed a subtle, wedgelike, dark gray lesion at the inferior fovea, which was better delineated with adjunct NIR imaging (Figure 2B and C). The registered SD-OCT through the lesion revealed a hyperreflective, plaquelike band at the junction of the OPL and INL that extended into the INL (Figure 2D and E), consistent with a type 1 lesion. The IS/OS was entirely intact,

and the OS/RPE appeared attenuated because of a shadowing effect from the type 1 lesion above.

Follow-up SD-OCT examination 4 months after the patient's initial presentation revealed a zone of severe INL thinning and markedly attenuated OPL where the hyperreflective lesion had been previously located (Figure 2 G and H). The deeper HFL had lost its optical reflex and appeared hyporeflective compared with the surrounding unaffected HFL. In addition, the dark lesion on NIR, as well as the shadowing it induced on SD-OCT, had dissipated (Figure 2F). The patient's BCVA remained 20/25 OD, and the scotoma persisted, although it had decreased in size.

### Case 2

A 65-year-old African American woman presented with a 1-week history of paracentral scotoma that she described as a "purplish pair of ragged lips" affecting her left eye. She denied any other visual symptoms or precipitating illnesses and had no significant medical history.

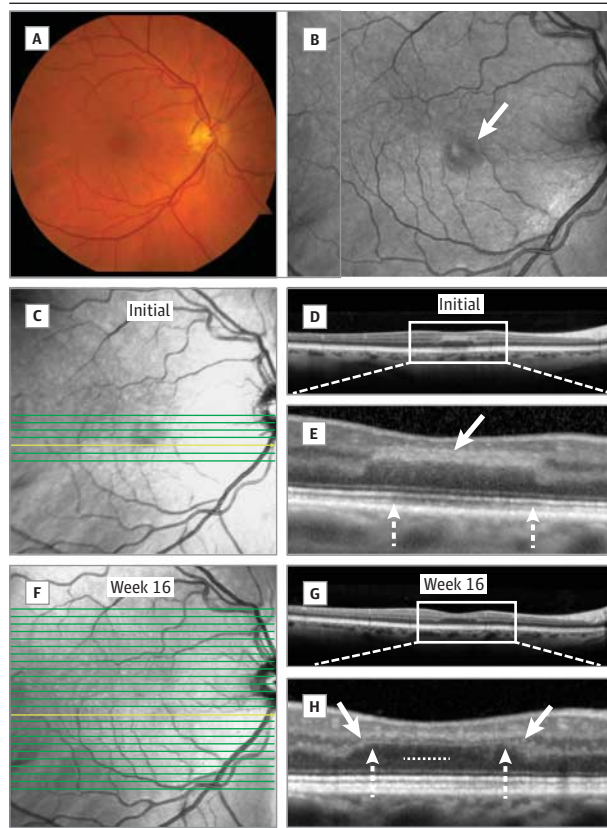
Her BCVA was 20/20 in the symptomatic left eye, whereas the fellow eye had a history of posterior staphyloma and amblyopia, with a BCVA of 20/60. The results of the remainder of her clinical examination were within normal limits. However, NIR imaging and near-infrared autofluorescence uncovered a dark, well-demarcated, nummular lesion at the nasal fovea in the left eye (Figure 3A and B). As in the previous case, the SD-OCT scan through this dark area revealed a hyperreflective band at the junction of the OPL and INL that extended into the INL (Figure 3C), consistent with a type 1 lesion, which similarly induced a shadowing effect on the deeper retinal layers. The IS/OS band was entirely intact.

The patient was followed up closely with serial SD-OCT examinations performed up to 30 weeks after the initial presentation (Figure 3D-G and J). The sequential scans demonstrated gradual resolution of the hyperreflective lesion, with subsequent progressive atrophy and severe thinning of the involved OPL and INL. These resulting atrophic changes induced a partial collapse of the overlying retinal structures, leading to the irregular foveal architecture observed, which was best appreciated on the final scan 30 weeks later (Figure 3J). At that visit, the visual acuity in the affected eye was stable at 20/20, and the NIR and NIA images were unremarkable (Figure 3H and I). As in the previous case, the underlying HFL again appeared to have lost its optical reflex and was hyporeflective relative to the normal adjacent HFL.

### Case 3

A 56-year-old white man was referred for evaluation of paracentral scotomas in the left eye greater than the right eye of 6 weeks' duration. Several days before the onset of his symptoms, he underwent a total left hip arthroplasty with an operative time of 6 hours, during which he required transfusion of 2 U of packed red blood cells because of severe blood loss. The patient had a complicated postoperative course that necessitated prolonged inpatient hospitalization. It was unknown whether he received pressor support during this period. Otherwise, his medical history was noncontributory.

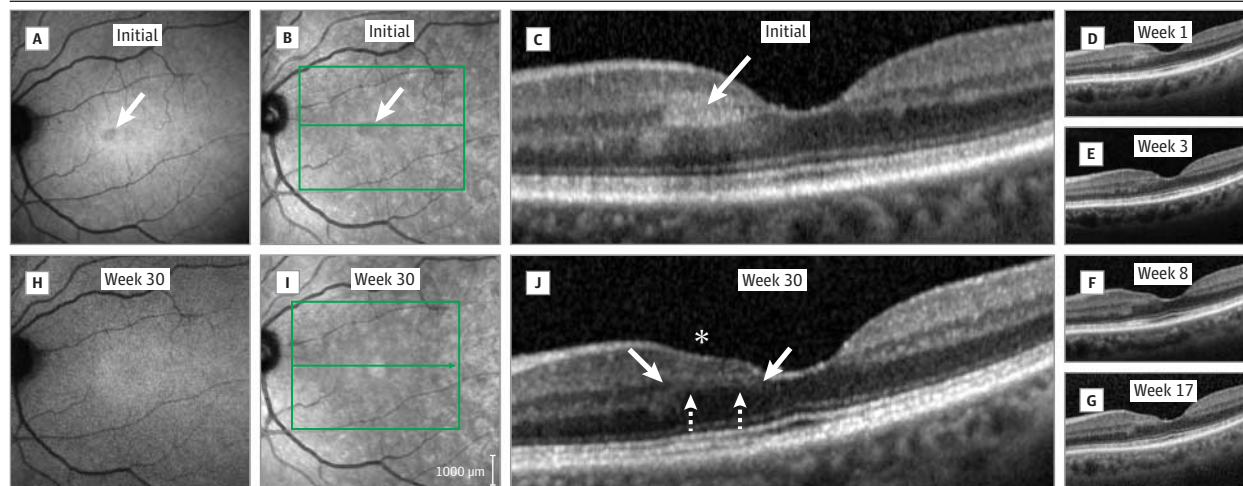
Figure 2. Case 1



A, Baseline color ophthalmoscopic image of the right eye that was normal. Red-free (B) and near-infrared (NIR) reflectance (C) images of the right eye revealed a subtle, dark gray, wedge-like lesion that involved the inferior fovea (arrow). D and E, Spectral domain optical coherence tomography (SD-OCT) through the lesion revealed a hyperreflective plaque at the junction of the outer plexiform layer (OPL) and inner nuclear layer (INL) that extended into the INL (arrow), consistent with a type 1 lesion. The inner segment/outer segment and outer segment/retinal pigment epithelium bands appeared hyporeflective beneath the lesion because of a shadowing effect (between interrupted arrows). At 16-week follow-up, the dark lesion on NIR had dissipated (F) and SD-OCT (G and H) revealed a zone of severe INL thinning (between top solid arrows) and markedly attenuated OPL (between bottom interrupted arrows), where the hyperreflective lesion had been previously located. Notably, the deeper Henle fiber layer had lost its optical reflex and now appeared hyporeflective (space between small dotted line and OPL), whereas the shadowing of the outer layers had resolved.

At the time of his presentation, BCVA was 20/15 OD and 20/25 OS. Slitlamp examination was quiet bilaterally, and ophthalmoscopic examination findings were unremarkable with the exception of small macular drusen in both eyes (Figure 4A and J). The RF photographs demonstrated faint, irregular macular lesions bilaterally, greater in the left eye (Figure 4B and K). These paracentral lesions were dark and more discretely visible with NIR reflectance, with an arrangement that resembled a cloverleaf or petaloid pattern, particularly in the left eye (Figure 4C and L). Spectral domain optical coherence tomography performed at the initial presentation revealed perifoveal hyperreflectivity of the OPL and INL with normal IS/OS and OS/RPE bands (Figure 4, E, F, and N), consistent with a type 1 lesion. The results of supplemental FA and full-field electroretinography testing were normal.

Figure 3. Case 2



Baseline near-infrared autofluorescence (NIA) (A) and near-infrared (NIR) reflectance (B) demonstrated a dark, well-demarcated, nummular lesion at the nasal fovea in the left eye (arrows). C, Spectral domain optical coherence tomography (SD-OCT) through the lesion revealed a hyperreflective band at the junction of the outer plexiform layer (OPL) and inner nuclear layer (INL) that extended into the INL (arrow), consistent with a type 1 lesion, which induced a shadowing effect on the deeper retinal layers. D, E, F, G, and J, Serial SD-OCT examinations performed up to 30 weeks after the initial presentation revealed

gradual resolution of the hyperreflective lesion along with the shadowing effect it created, as well as progressive atrophy and severe thinning of the involved OPL (between bottom interrupted arrows) and INL (between top solid arrows). The atrophic changes induced a partial collapse of the overlying retinal structures, leading to the irregular foveal architecture observed (asterisk). Notably, the deeper Henle fiber layer had lost its optical reflex and now appeared hyporeflective (dark space between bottom interrupted arrows). Follow-up NIR (H) and NIA (I) images were unremarkable for any abnormalities.

Seven weeks later, the patient's subjective symptoms had improved. His BCVA was stable at 20/15 OD and had improved to 20/20 OS. With NIR reflectance, the macular lesions were lighter and less distinct (Figure 4G and O). The correlating SD-OCT scans revealed that the hyperreflectivity of the OPL and INL, although still present in both eyes, had decreased in size and intensity (Figure 4H, I, and P).

#### Case 4

A 60-year-old white man presented with a 2-day history of paracentral scotoma in the right eye. He reported having symptoms consistent with a flulike illness approximately 1 week prior. The remainder of his medical history was noncontributory.

His BCVA was 20/20 OU at the time of evaluation. Ophthalmoscopic examination of the symptomatic right eye revealed an ill-defined intraretinal white lesion (Figure 5A), which appeared similar with RF photography (Figure 5B). However, with NIR reflectance, the lesion appeared dark and more precisely delineated (Figure 5C). The SD-OCT imaging through the defect revealed a hyperreflective plaque at the junction of the OPL and INL that extended into the INL (Figure 5D), which cast a shadow over the outer retinal layers, consistent with a type 1 lesion. The IS/OS and OS/RPE bands were entirely intact.

Four weeks later, the patient returned and had improved symptomatically, although his BCVA remained stable at 20/20 OD. On follow-up NIR imaging, the dark lesion had dissipated (Figure 2E). Corresponding SD-OCT revealed a zone of severe INL thinning and an irregular, attenuated OPL (Figure 5F). The HFL underlying this OPL appeared hyporeflective compared

with the adjacent unaffected HFL, similar to patients 1 and 2. Meanwhile, the shadowing of the outer retinal layers had resolved.

#### Case 5

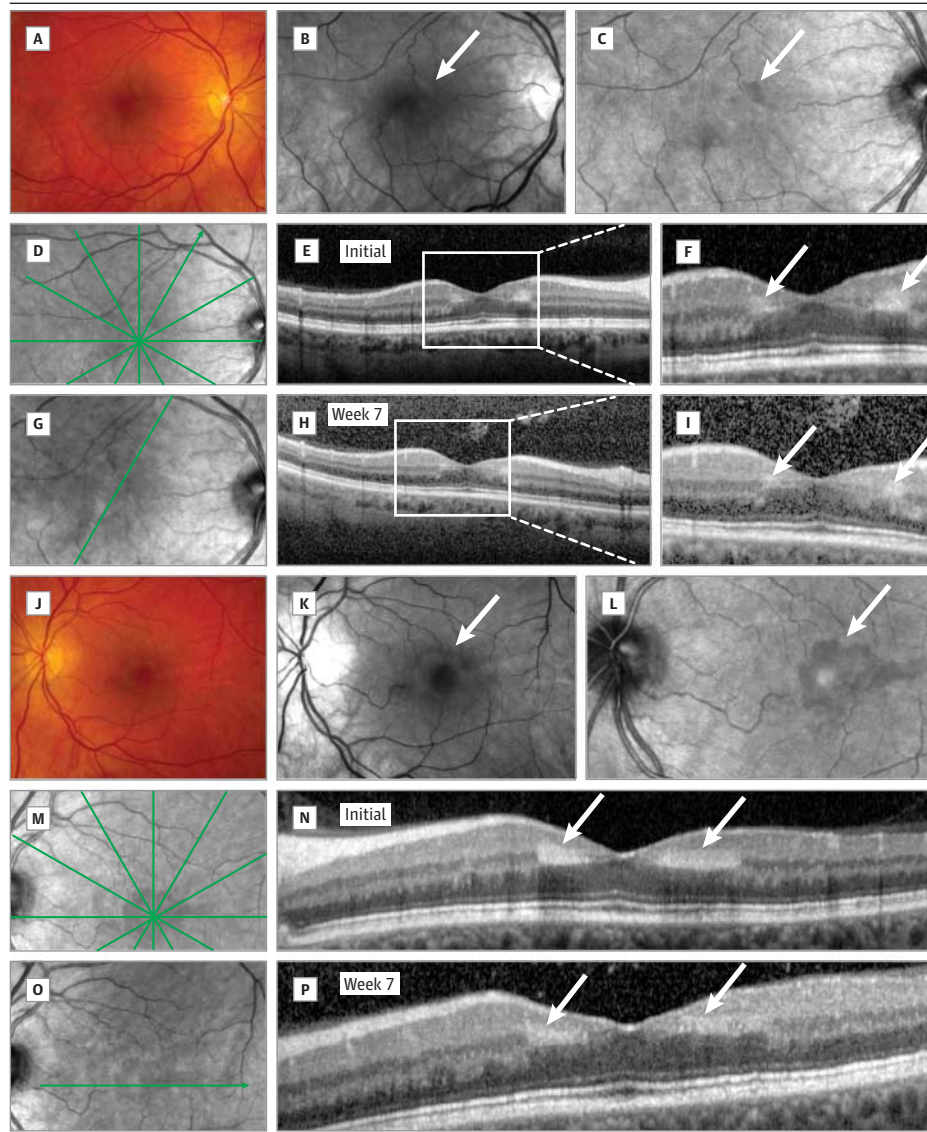
A 54-year-old Middle Eastern man presented with a 2-day history of an inferonasal paracentral scotoma in the left eye. He denied any antecedent flulike prodromal illness and was otherwise healthy.

His BCVA was 20/20 OU at the time of evaluation. Anterior segment examination results were within normal limits, but ophthalmoscopy of the left eye revealed a paracentral superotemporal intraretinal white lesion associated with a subtle intraretinal hemorrhage (Figure 6A). The remainder of the retinal examination findings were only remarkable for a few small macular drusen bilaterally. The RF photography helped better demarcate the borders of the white lesion (Figure 6B). Corresponding FA revealed a subtle blocking defect over the focus of the intraretinal hemorrhage (Figure 6C) but other findings were otherwise unremarkable.

With NIR reflectance, the lesion appeared dark, with its borders more sharply outlined (Figure 6D). The registered SD-OCT image through the defect revealed a hyperreflective plaque at the junction of the OPL and INL that extended into the INL (Figure 6E), which cast a shadow over the outer retinal layers, consistent with a type 1 lesion. The IS/OS and OS/RPE bands were entirely intact.

Two weeks later, the patient returned and had improved symptomatically, whereas his BCVA remained stable at 20/20 OS. On follow-up NIR imaging, the dark lesion appeared lighter

Figure 4. Case 3



Baseline color ophthalmoscopic (A and J), red-free (B and K), and near-infrared (NIR) reflectance (C, D, L, and M) images of both eyes demonstrated cloverleaf or flower-petal-shaped macular lesions (arrows) greater in the left than right eye. Spectral domain optical coherence tomography (SD-OCT) (E, F, and N) revealed perifoveal hyperreflectivity of the outer plexiform layer (OPL) and inner nuclear layer (INL) (arrows) with normal inner segment/outer segment and outer segment/retinal pigment epithelium bands, consistent with a type 1 lesion. At 7-week follow-up, the lesions were lighter and less distinct on NIR (G and O). Corresponding SD-OCT (H, I, and P) revealed that the hyperreflectivity of the OPL and INL, although still present in both eyes, had decreased in size and intensity (arrows).

and less distinct than previously (Figure 6F). Similarly, the SD-OCT hyperreflective band was still present, although not as intense as it appeared on presentation (Figure 6G) and with associated thinning of the INL. The shadowing of the outer retinal layers had also resolved.

### Case 6

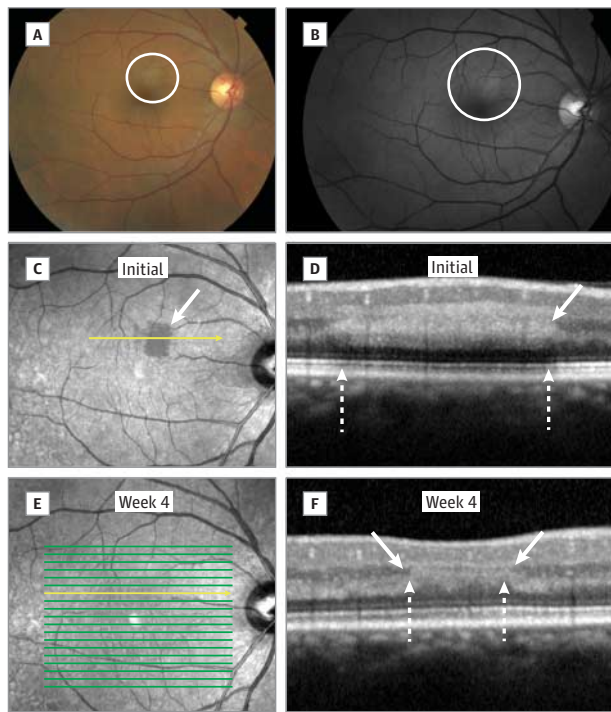
A 33-year-old white woman was referred for a 5-day history of a central “spot” in her left eye. She denied any antecedent flu-like illness and was not taking any medications. Her medical history was significant for a previous episode of toxic shock syndrome.

Her BCVA at presentation was 20/20 OU. Ophthalmoscopic examination of the left eye revealed a pale, semitranslucent, teardrop-shaped lesion in the parafoveal region associated with a focus of intraretinal hemorrhage at its base (Figure 7A). A blocking defect secondary to the intraretinal heme was confirmed by FA, but otherwise the FA results were

unremarkable (Figure 7B). The NIR reflectance better outlined the borders of the teardrop lesion, which appeared dark with this imaging modality (Figure 7C). The registered SD-OCT through the lesion revealed a hyperreflective band at the level of the OPL and ONL, with attenuation of the underlying IS/OS and OS/RPE layers (Figure 7D), consistent with a type 2 lesion.

The patient was still symptomatic at her 2-month follow-up visit, whereas her BCVA remained intact at 20/20 OU. The pale lesion was no longer detectable by ophthalmoscopic examination, color photography, or FA, and the intraretinal hemorrhage had resolved (Figure 7, E and F). However, NIR imaging confirmed persistence of the lesion, although it appeared less prominent compared with the image obtained at her initial visit (Figure 7G). The SD-OCT revealed that the hyperreflective area had resolved, with subsequent thinning of the ONL overlying an attenuated IS/OS and OS/RPE complex (Figure 7H).

Figure 5. Case 4



Baseline color ophthalmoscopic (A) and red-free (B) images of the right eye revealed an ill-defined intraretinal white lesion, which appeared dark and well circumscribed (arrow) with near-infrared (NIR) reflectance (C). D, Spectral domain optical coherence tomography (SD-OCT) through the lesion demonstrated a hyperreflective band (arrow) at the junction of the outer plexiform layer (OPL) and inner nuclear layer (INL) that extended into the INL, consistent with a type 1 lesion. This lesion produced a shadow over the outer retinal layers (between interrupted arrows). E, At 4-week follow-up, the lesion was no longer detectable on NIR. F, Corresponding SD-OCT revealed a zone of severe INL thinning (between top solid arrows) and an irregular, attenuated OPL (between bottom interrupted arrows), where the hyperreflective lesion had been previously located. The Henle fiber layer underneath the OPL now appeared moderately hyporeflective compared with the surrounding unaffected HFL, whereas the shadowing effect on the deeper retinal layers had resolved.

### Case 7

A previously healthy 43-year-old white woman presented with a 4-day history of a paracentral scotoma she described as a “claw-shaped gray area” just temporal to fixation in her right eye. On examination, her BCVA was 20/20 OU. Ophthalmoscopy of the symptomatic right eye revealed a paracentral, well-demarcated, wedge-shaped opacification nasal to fixation in the right eye that was more obvious with RF photography (Figure 8A-C). This lesion appeared dark with NIR reflectance imaging (Figure 8D). With high-magnification FA, a focal area of microvascular remodeling involving the nasal foveal capillary network and directly adjacent to the visible macular lesion was noted (Figure 8E-G). Microperimetry confirmed corresponding functional visual loss in this region (Figure 8H). The corresponding SD-OCT through the lesion revealed a hyperreflective band that involved the OPL and ONL with associated disruption of the IS/OS and OS/RPE layers (Figure 8I and J), consistent with a type 2 lesion.

One week later, the patient’s symptoms were unchanged. By this time, the lesion was no longer visible on examination

or with color photography; however, it was still detectable with NIR imaging. Subsequent SD-OCT revealed a slight decrease in size of the hyperreflective lesion within the OPL and ONL with continued disruption of the IS/OS and OS/RPE lines (Figure 8K).

After 2 weeks, her symptoms were still present, but the lesion appeared smaller and less dark with NIR imaging. The SD-OCT revealed a progressive decrease in size and intensity of the hyperreflective band with patchy restoration of the IS/OS and OS/RPE layers in areas in which the hyperreflectivity had resolved (Figure 8L).

At her 1-month clinic visit, the patient reported that the symptoms were gradually improving, and her visual acuity remained stable at 20/20 OU. The lesion was no longer detectable with NIR imaging and had nearly resolved with SD-OCT, which demonstrated persistence of punctate hyperreflective areas within the OPL and ONL. By this time point, the IS/OS and OS/RPE bands had been restored (Figure 8M).

### Case 8

A 35-year-old white woman primigravid with twins was admitted during the 33rd week of pregnancy for observation and treatment of preeclampsia. Her blood pressure on admission was 150/90 mm Hg and became increasingly difficult to manage during the hospitalization, necessitating early induction of labor. Shortly after, the patient began to experience “blurred vision” in both eyes, prompting an inpatient ophthalmology consultation.

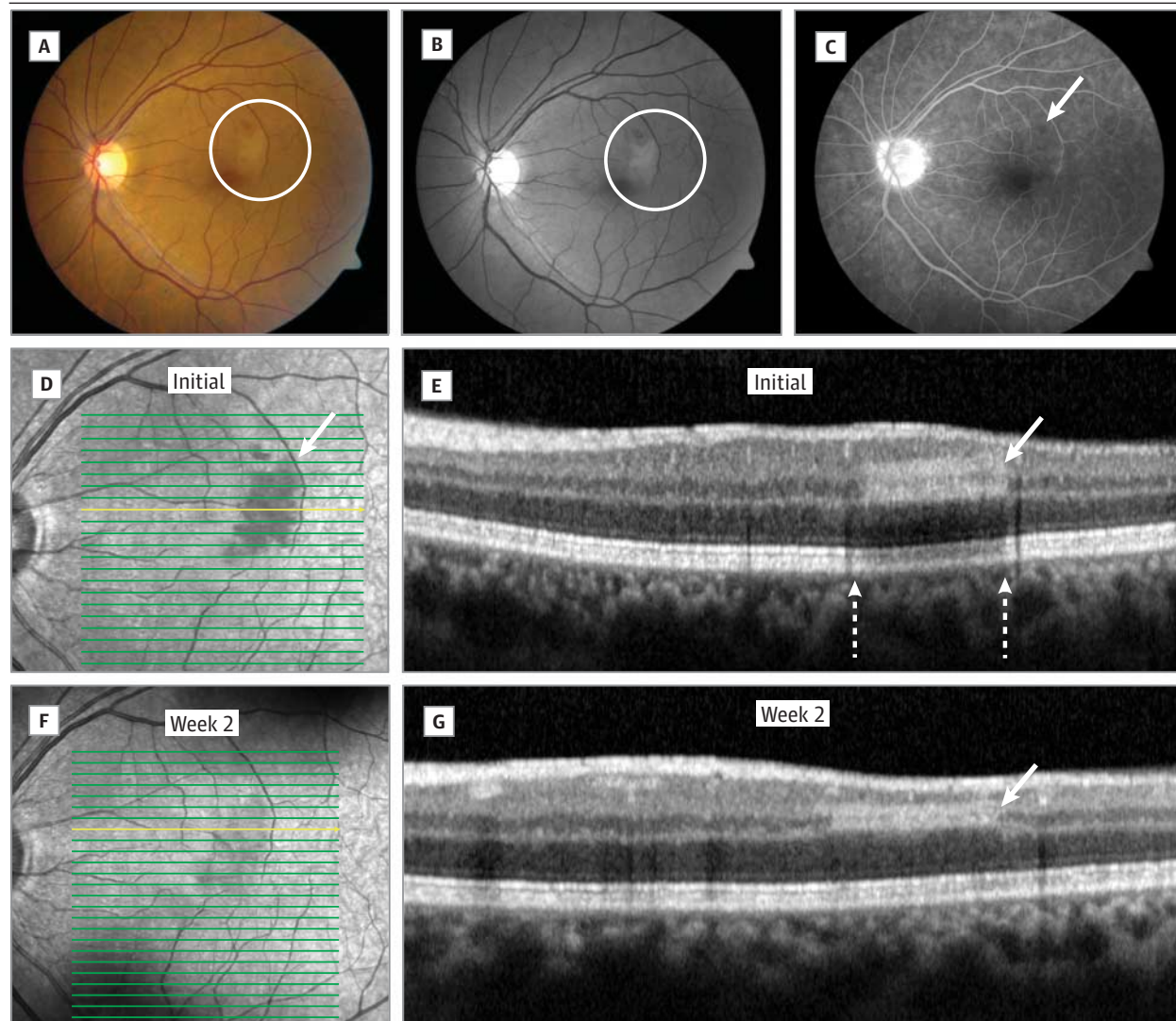
Her BCVA was 20/25 OD and 20/30 OS at the time of evaluation. Amsler grid testing revealed a central scotoma in the left eye. Anterior segment examination results were within normal limits. Ophthalmoscopy demonstrated bilateral cotton-wool spots and red-brown discoloration of the central macula, greater in the left eye than in the right eye (Figure 9A and I). The NIR imaging revealed bilateral, well-demarcated, petaloid-shaped, dark gray macular lesions (Figure 9B and J). The SD-OCT corresponding to these areas revealed involvement of the HFL and ONL and patchy dropout of the IS/OS and OS/RPE lines in the right eye and pronounced attenuation of both layers in the left eye consistent with bilateral type 2 lesions (Figure 9C, D, K, and L). The results of FA were only remarkable for late, faint hyperfluorescent areas corresponding to the cotton-wool spots seen clinically (Figure 9E and M).

One month later, the patient thought her vision was improved but not yet back to baseline. Her BCVA was stable, and the scotoma in her left eye had decreased in density. Follow-up NIR imaging revealed persistence of the macular lesions, although the lesions appeared less intense with less distinct margins (Figure 9F and N). On SD-OCT, there was notable atrophy and thinning of the ONL bilaterally, and although the IS/OS and OS/RPE layers were still largely compromised, both eyes demonstrated patches of regenerating IS/OS (Figure 9G, H, O, and P).

### Case 9

A previously healthy 21-year-old white woman was referred for evaluation of a central “bright spot” in the left eye for the previous 18 days. She had already been seen by a local retina specialist and neuro-ophthalmologist before her presenta-

Figure 6. Case 5



Baseline color ophthalmoscopic (A) and red-free (B) images of the left eye revealed an ill-defined intraretinal white lesion with an associated intraretinal hemorrhage and few small macular drusen. C, Corresponding fluorescein angiography confirmed a subtle blocking defect over the focus of intraretinal hemorrhage (arrow), but findings were otherwise unremarkable. D, With near-infrared (NIR) reflectance, the lesion now appeared dark and well-circumscribed (arrow). E, Spectral domain optical coherence tomography (SD-OCT) through the lesion demonstrated a hyperreflective band (arrow) at

the junction of the outer plexiform layer and inner nuclear layer (INL) that extended into the INL, consistent with a type 1 lesion. This lesion produced a shadow over the outer retinal layers (between interrupted arrows). At 2-week follow-up, the NIR lesion (F) appeared lighter and less distinct than previously, whereas the SD-OCT hyperreflective band (G) was still present (arrow), although not as intense as it appeared on presentation with associated thinning of the INL. The shadowing of the outer retinal layers had also resolved.

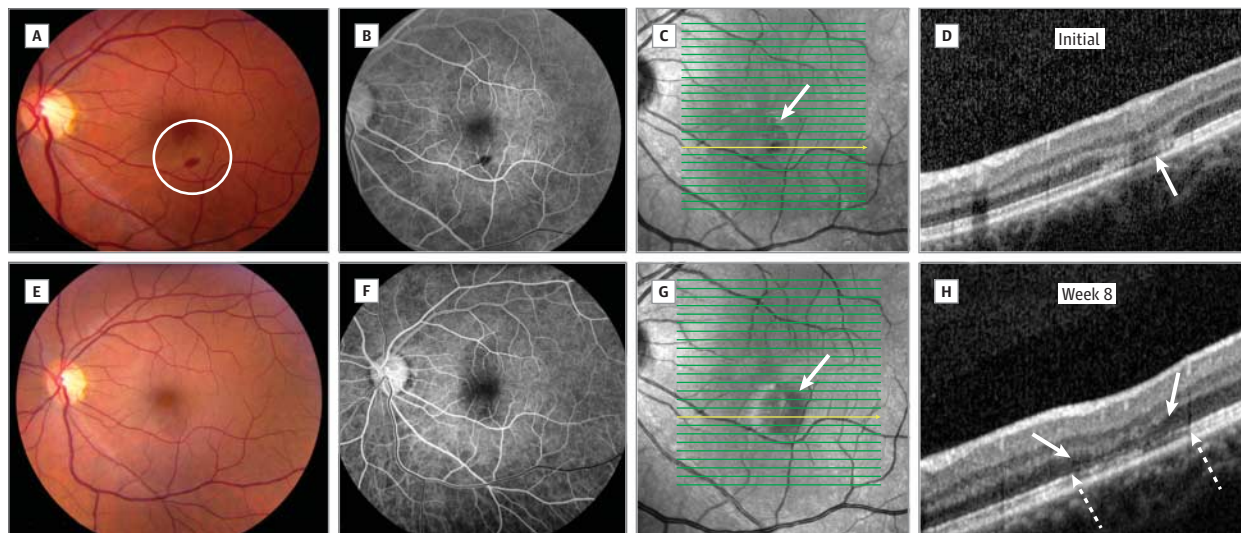
tion and was told that the results of her ophthalmologic examination were normal.

Her BCVA was 20/20 OD and 20/25 OS. Anterior segment and retinal examination findings were grossly unremarkable, but color ophthalmoscopic imaging of the left eye revealed a barely detectable dark paracentral lesion (Figure 10A). The NIR reflectance of the left eye uncovered a small, wedge-shaped, dark-gray lesion that involved the superotemporal fovea (Figure 10B). The SD-OCT corresponding to the NIR defect revealed a subtle hyperreflective lesion that involved the OPL and ONL with associated focal disruption of the IS/OS and OS/RPE layers (Figure 10, D and E), which was consistent with a type 2 lesion.

A montage of 3 images of the left eye was acquired with the rtx1 AO retinal camera (Figure 10C). The dark lesion visualized on the NIR image corresponded to an area where fewer cones were visualized in the AO montage. Notably, the area of disruption of the cone mosaic on the AO montage was more widespread (Figure 10C) than the lesion visualized on the NIR image (Figure 10B). The cone mosaic reflectivity, contiguity, and spacing around the lesion appeared normal (no quantitative evaluation performed).

Three weeks later, the patient returned and had improved symptomatically, whereas the BCVA remained unchanged. Follow-up SD-OCT revealed partial reconstitution of the IS/OS and OS/RPE layers.

Figure 7. Case 6



A, Baseline color ophthalmoscopic image of the left eye revealed a pale, semitranslucent, teardrop-shaped lesion in the parafoveal region associated with a focus of intraretinal hemorrhage at its base. B, Fluorescein angiography (FA) confirmed a blocking defect secondary to the intraretinal heme but was otherwise unremarkable. C, Near-infrared (NIR) reflectance better outlined the borders of the dark teardrop lesion (arrow). D, Spectral domain optical coherence tomography (SD-OCT) through the lesion revealed a hyperreflective band at the level of the outer plexiform layer and outer nuclear layer (ONL) (arrow) with attenuation of the underlying inner segment/outer segment

(IS/OS) and outer segment/retinal pigment epithelium (OS/RPE) layers, consistent with a type 2 lesion. At 8-week follow-up, the pale lesion was no longer detectable by color photography (E) or FA (F), and the intraretinal hemorrhage had resolved; however, NIR (G) confirmed persistence of the lesion, although it appeared less prominent compared with the baseline examination (arrow). H, SD-OCT revealed that the hyperreflective area had resolved with subsequent thinning of the ONL (between top solid arrows) overlying an attenuated IS/OS (left-most interrupted arrow) and OS/RPE (right-most interrupted arrow) complex.

## Results

The Table provides a detailed summary of the clinical data for each patient. Although type 1 lesions lead to thinning of the INL, type 2 lesions lead to thinning of the ONL. Type 2 lesions were always associated with significant outer macular defects, including obvious attenuation of the IS/OS and OS/RPE bands, whereas type 1 lesions failed to disrupt the integrity of the IS/OS junction. In our study, 6 eyes (patients 1-5) had type 1 lesions and 5 eyes (patients 6-9) had type 2 lesions. Note that although there was a significant age and sex difference between the 2 groups and a different level of OCT involvement, the demographic and clinical findings between the 2 groups were similar and consistent with the diagnosis of AMN for each case. Nevertheless, we have elected to describe type 1 lesions as a paracentral acute middle maculopathy to reflect the unique SD-OCT level of disease (Table).

## Discussion

More sophisticated imaging systems have helped to redefine the clinical presentation of AMN and have markedly enhanced diagnostic sensitivity. In some cases of AMN, ophthalmoscopic abnormalities may be entirely absent, and color ophthalmoscopic photography findings may be essentially normal, as in patients 1, 2, 3, and 9 in our study. Greater diagnostic reliance has shifted toward the use of NIR reflectance imaging

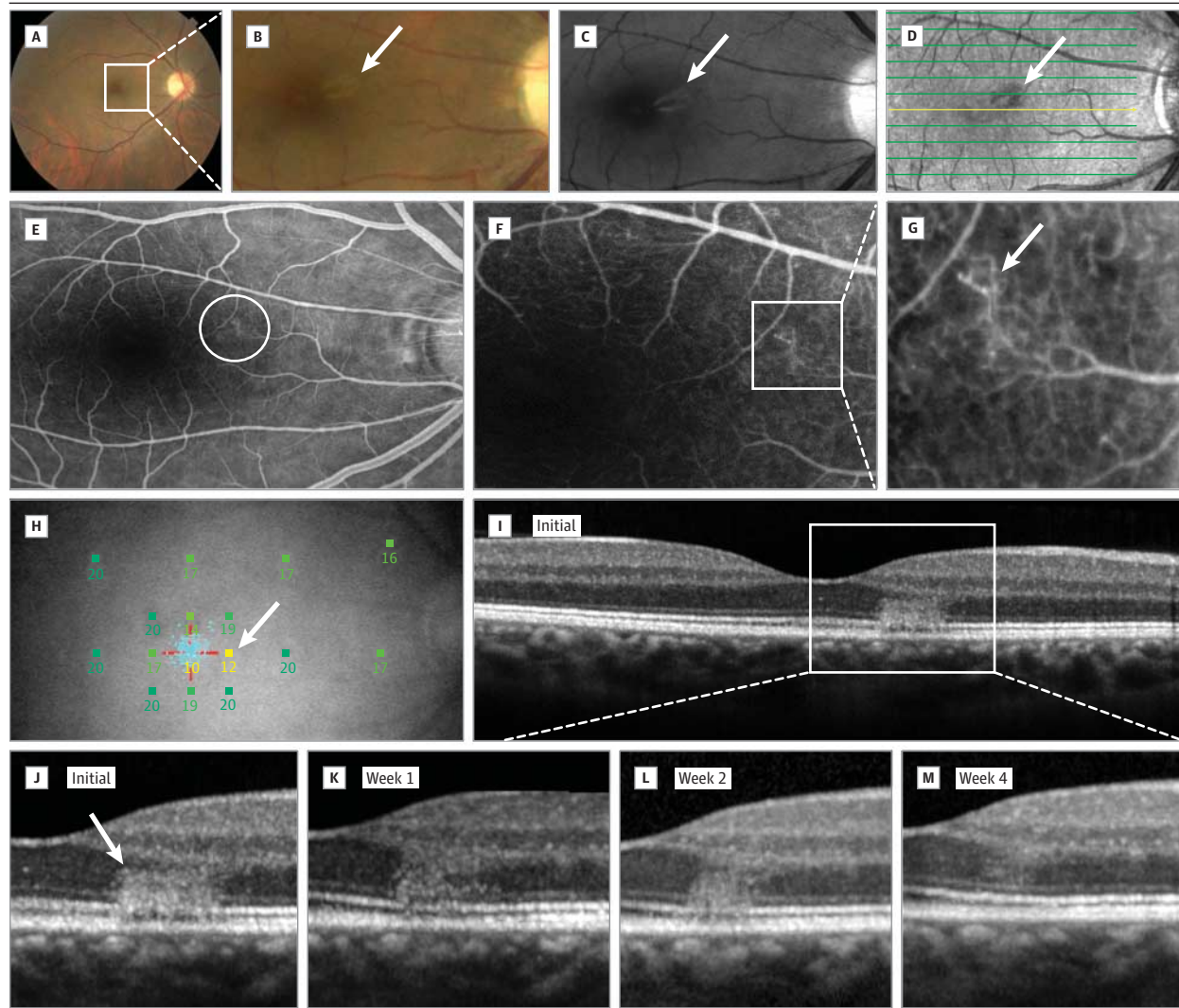
to demonstrate characteristic dark gray paracentral lesions that typically point toward the foveal center.<sup>4,7-9</sup> The SD-OCT may reliably detect outer macular abnormalities, including IS/OS and OS/RPE loss and ONL thinning.<sup>3,4,10</sup>

Recently, various authors<sup>4,7</sup> have discovered that AMN lesions may develop at the junction of the OPL/ONL zones with associated outer macular disruption. It is apparent from this study that AMN lesions may even involve the middle layers of the retina at the junction of the OPL and INL zones, a novel SD-OCT presentation that we referred to as a paracentral acute middle maculopathy. We identified 6 eyes with middle SD-OCT lesions above the OPL (type 1) and 5 eyes with outer SD-OCT lesions below the OPL (type 2).

Each lesion type may possibly be explained by retinal capillary ischemia. In postmortem studies on human donor eyes, Tan et al<sup>11</sup> identified 4 different capillary networks in the human retina located in the following regions: nerve fiber layer, retinal ganglion cell layer, junction of the inner plexiform layer and superficial boundary of the INL (ie, the SCP), and junction of the deep INL and OPL (ie, the DCP) border. In our study all type 1 lesions were noted on SD-OCT to extend from the border of the OPL to the most superficial edge of the INL, with subsequent thinning of the INL. These type 1 lesions are precisely aligned with the SCP (Figure 11), and given the vasculopathic risk factors associated with our patients with type 1 lesions, we propose that occlusion of the SCP is the likely origin for these lesions.

By contrast, type 2 lesions of the OPL/ONL region are more closely aligned with the DCP. The OPL is composed of photo-

Figure 8. Case 7



Baseline color ophthalmoscopic (A and B) and red-free (C) images revealed a paracentral, well-demarcated, wedge-shaped opacification nasal to fixation in the right eye. D, This lesion appeared dark with near-infrared reflectance. Routine (E) and high-magnification fluorescein angiography (F and G) denoted a focal area of microvascular remodeling involving the nasal foveal capillary network and directly adjacent to the visible macular lesion. H, Microperimetry confirmed corresponding functional visual loss in this region (arrow). I and J, Spectral domain optical coherence tomography (SD-OCT) revealed a

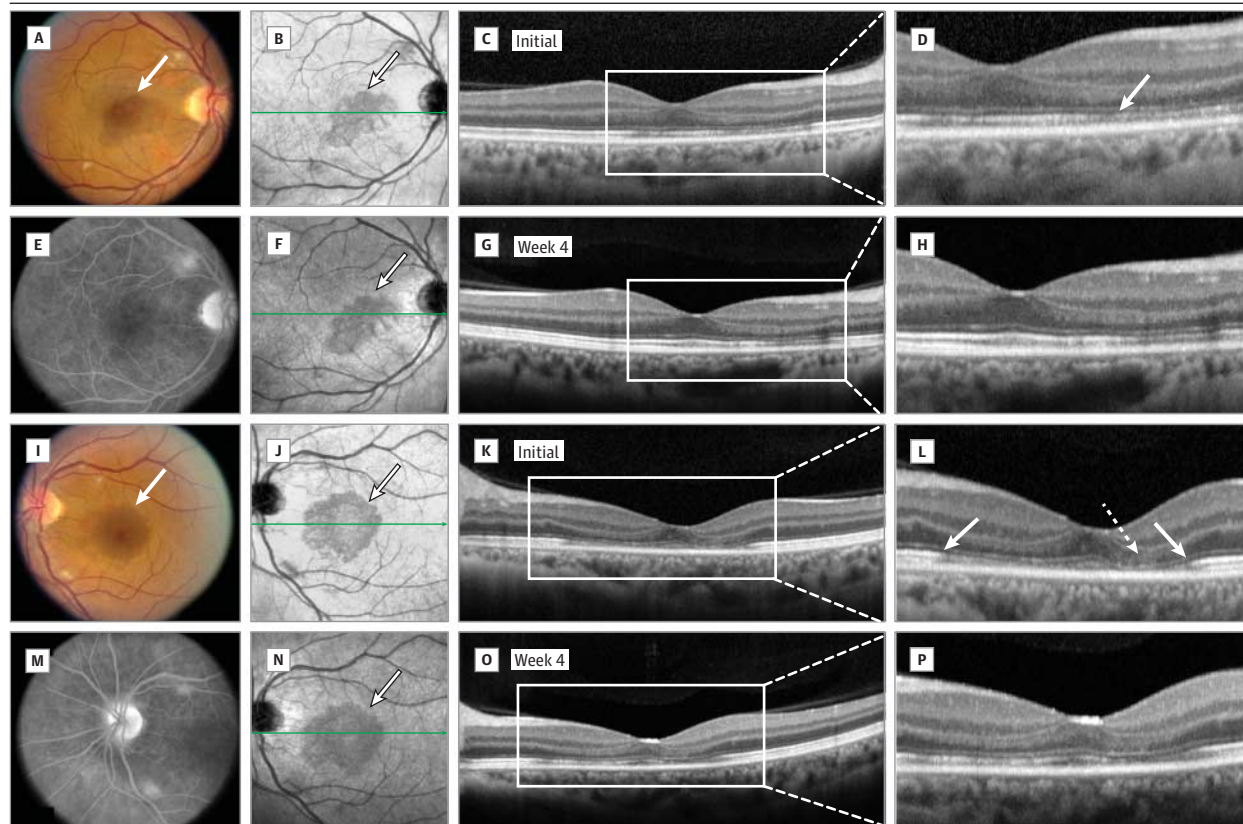
hyperreflective band that involved the outer plexiform layer (OPL) and outer nuclear layer (ONL) (arrow) with associated disruption of the inner segment/outer segment (IS/OS) and outer segment/retinal pigment epithelium (OS/RPE) layers, consistent with a type 2 lesion. K, L, and M, Serial SD-OCT scans displayed gradual resolution of the hyperreflectivity with persistence of punctate hyperreflective areas within the OPL and ONL, whereas the IS/OS and OS/RPE lines were restored.

receptor axon terminals, and this layer lies directly adjacent to the DCP located in the outermost portion of the INL (Figure 11). In the foveal and perifoveal areas, the HFL occupies a significant portion of the outer OPL.<sup>12</sup> The DCP provides 10% to 15% of the oxygen supply to the photoreceptor population.<sup>13</sup> The photoreceptor axon terminals are replete with oxygen-dependent mitochondria as demonstrated by Stone et al<sup>14</sup> and may rely more heavily on the DCP for oxygen supply than the photoreceptor inner and outer segments located closer to the underlying choriocapillaris. A steady decrease of the diffusion gradient of oxygen from the choriocapillaris to the photoreceptor axons has been experimentally confirmed by Wangsa-Wirawan et al.<sup>15</sup> As such, the

OPL and the region immediately below the OPL may act as a watershed zone and may be especially vulnerable to ischemic insults to the DCP. Subsequent axonal and outer segment disruption and death may develop as evidenced by the IS/OS and OS/RPE abnormalities that develop with type 2 lesions (patients 6-9) on SD-OCT and is further confirmed by the presence of cone loss illustrated by AO imaging in patient 9.

It is well known that AMN is a disorder associated with various pressor agents or vasoconstrictors, including sympathomimetics, such as epinephrine,<sup>16-19</sup> norepinephrine,<sup>20</sup> ephedrine,<sup>16</sup> or caffeine.<sup>21</sup> It is possible that the use of sympathomimetics, as in patient 1 who admitted to heavy caf-

Figure 9. Case 8



Baseline color ophthalmoscopic (A and I) images of both eyes showed bilateral cotton-wool spots and reddish brown discoloration of the central macula, greater in the left than right eye (arrows), which appeared as dark gray, well-demarcated, petaloid-shaped macular lesions on near-infrared (NIR) reflectance (B and J, arrows). E and M, Fluorescein angiography displayed late, faint hyperfluorescence of the cotton-wool spots seen clinically. Corresponding spectral domain optical coherence tomography (SD-OCT) (C, D, K, and L) revealed patchy dropout of the inner segment/outer segment (IS/OS) and outer segment/retinal pigment epithelium (OS/RPE) bands in the right eye (D, arrow)

and pronounced attenuation of both layers in the left eye (L, between solid arrows). L, A subtle hyperreflective lesion involving the Henle fiber layer and the outer nuclear layer (ONL) was observed in conjunction with an attenuated ONL, more prominently in the left eye (interrupted arrow), which was consistent with a type 2 lesion. F and N, At 4-week follow-up, NIR imaging revealed less intense macular lesions with less distinct margins (arrows). G, H, O, and P, On SD-OCT there was notable atrophy of the ONL bilaterally, and although IS/OS and OS/RPE layers were still largely compromised, both eyes demonstrated patches of regenerating IS/OS.

feine intake, may induce vasoconstriction of the SCP, leading to ischemia and development of the hyperreflective OPL/INL band (type 1 lesion) associated with AMN. Similar type 1 lesions developed bilaterally in patient 3, perhaps because of systemic hypotension and severe blood loss causing ischemia of the SCP. Thinning of the INL and ONL that ensues with type 1 and 2 lesions, respectively, appears to be a long-standing change that further reinforces the ischemic theory.

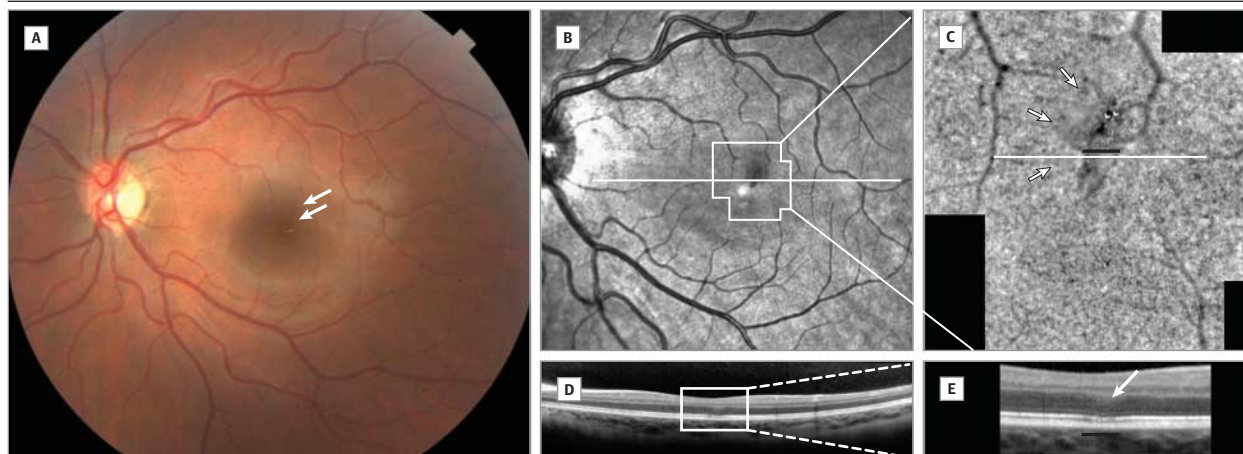
Retinal capillary ischemia is further supported by the presence of a dilated DCP as demonstrated by high-magnification FA in patient 7. Moreover, some cases of AMN may demonstrate an isolated intraretinal retinal hemorrhage<sup>22,23</sup> in association with the wedge-shaped AMN lesion as illustrated in patients 5 and 6, further supporting a vascular occlusive or vasculopathic origin. In addition, patient 8 had classic paracentral petaloid NIR lesions diagnostic of AMN, likely the result of toxemia of pregnancy and associated hypertension. This patient also demonstrated cotton-wool spots due to occlusion of the precapillary arterioles and infarction of the inner

retina, and it is likely that the bilateral type 2 AMN lesions may be explained by capillary ischemia of the outer retina due to vaso-occlusion of the DCP.

If the ischemic insult is severe enough, photoreceptor and outer segment loss may ensue, as evidenced by OS/RPE and IS/OS defects (type 2 lesion) with SD-OCT and cone loss with AO imaging (patient 9). Ischemic infarcts may lead to permanent INL (type 1) or ONL (type 2) thinning and even outer segment loss (type 2) and may explain persistent paracentral field defects in some patients with AMN,<sup>4</sup> including all of our patients, although follow-up was limited in some cases. Other ischemic insults to the SCP or DCP may be potentiated by trauma,<sup>24</sup> shock,<sup>20,25</sup> hypotension,<sup>26</sup> or severe blood loss, as occurred in patient 3.

Limitations of our study include the retrospective nature of the case review and the small number (n = 11) of eyes studied, although this is one of the largest case series of AMN to date. Although we have provided clinical and anatomical evidence to support retinal capillary ischemia as the cause of AMN,

Figure 10. Case 9



A, Baseline color ophthalmoscopic image of the left eye revealed a barely detectable dark paracentral lesion (arrows). B, Near-infrared (NIR) reflectance uncovered this small, dark gray, wedge-shaped lesion that involved the superotemporal fovea (lesion surrounded by white box). Registered spectral domain optical coherence tomography (SD-OCT) (D and E) through NIR lesion (B, horizontal white line) revealed a subtle hyperreflective lesion that involved the outer plexiform layer and outer nuclear layer (E, arrow), with an associated focal disruption of the inner segment/outer segment and outer segment/retinal

pigment epithelium bands (E, above black line), consistent with a type 2 lesion. C, Adaptive optics (AO) imaging over the lesion revealed a zone where fewer cones were visualized. The area of disruption of the cone mosaic on AO was more widespread (white arrows) than the lesion visualized on the NIR image (black line). This poor visualization of the cones could correspond to an optical defect or to disruption of the cone outer segments. However, some cones were well visualized and bright within the dark area (white arrowheads), suggesting that their reduced number is not simply an optical defect.

Table. Patient Demographics and Examination Findings

Patient No./Sex/Age, y	Eye	Race	Risk Factors	BCVA	Scotoma	Ophthalmoscopic Photographs	NIR Lesion	SD-OCT Lesion
Type 1 lesions								
1/M/61	Right	White	Caffeine	20/25	Paracentral	Normal	Wedgelike, dark	OPL/INL
2/F/65	Left	African American	None	20/20	Paracentral	Normal	Nummular, dark	OPL/INL
3/M/56	Right	White	Blood loss	20/15	Paracentral	Normal	Petaloid, dark	OPL/INL
M/56	Left	White	Blood loss	20/25	Paracentral	Normal	Petaloid, dark	OPL/INL
4/M/60	Right	White	Viral prodrome	20/20	Paracentral	Ill-defined, white lesion	Wedgelike, dark	OPL/INL
5/M/54	Left	Middle Eastern	None	20/20	Paracentral	Ill-defined, white lesion with hemorrhage	Wedgelike, dark	OPL/INL
Type 2 lesions								
6/F/33	Left	White	None	20/20	Paracentral	Semitranslucent teardrop lesion with hemorrhage	Teardrop, dark	OPL/ONL, IS/OS, OS/RPE
7/F/43	Right	White	None	20/20	Paracentral	Wedgelike, white lesion	Wedgelike, dark	OPL/ONL, IS/OS, OS/RPE
8/F/35	Right	White	Toxemia of pregnancy	20/25	Paracentral	Red-brown macular discoloration	Petaloid, dark	HFL/ONL, IS/OS, OS/RPE
F/35	Left	White	Toxemia of pregnancy	20/30	Paracentral	Red-brown macular discoloration	Petaloid, dark	HFL/ONL, IS/OS, OS/RPE
9/F/21	Left	White	None	20/25	Paracentral	Subtle, wedgelike, dark gray lesion	Wedgelike, dark	OPL/ONL, IS/OS, OS/RPE

Abbreviations: AMN, acute macular neuroretinopathy; BCVA, best-corrected visual acuity; HFL, Henle fiber layer; INL, inner nuclear layer; IS, inner segment; NIR, near-infrared reflectance; ONL, outer nuclear layer; OPL, outer plexiform

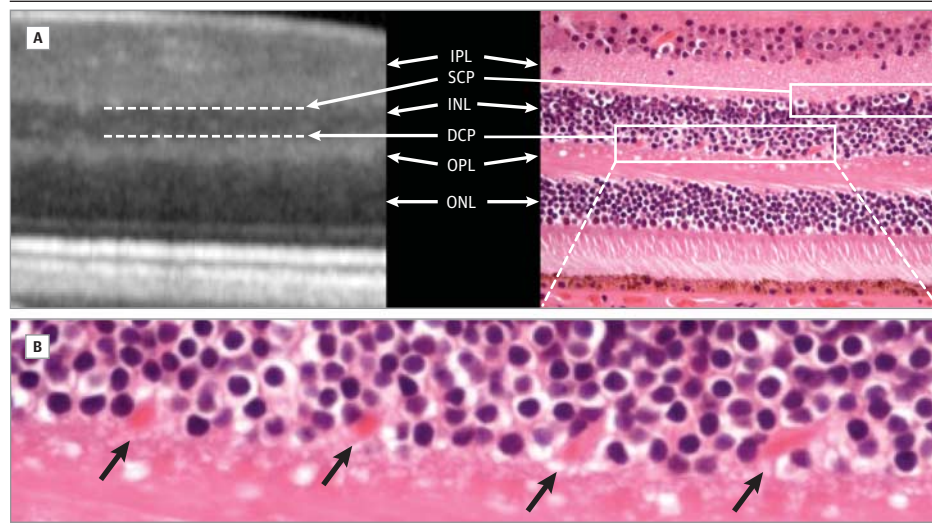
layer; OS, outer segment; RPE, retinal pigment epithelium; SD-OCT, spectral-domain optical coherence tomography.

this proposed mechanism has not yet been proven. Showing causality would require animal models of retinal capillary occlusion and subsequent demonstration of the characteristic findings of AMN with multimodal imaging.

The mean age of the 5 patients with type 1 lesions was 59.2 years (range, 54-65 years), whereas the 4 patients with type 2

lesions had a mean age of 33 years (range, 21-43 years). Moreover, patients with type 1 lesions tended to be male, whereas those with type 2 lesions tended to be female. Therefore, it is possible that the eyes that we have described as a paracentral acute middle maculopathy, or type 1 variant of AMN, may represent a novel macular disease altogether.

Figure 11. Histologic Analysis of the Superficial Capillary Plexus (SCP) and Deep Capillary Plexus (DCP)



A, Spectral domain optical coherence tomography (SD-OCT) and histologic correlate of a normal macula demonstrating the location of the SCP (top interrupted line) and DCP (bottom interrupted line) along the apical and basal surfaces of the inner nuclear layer (INL), respectively. B, Magnified histologic view of the microvascular network (black arrows). The black arrows denote individual vascular units of the DCP. IPL indicates inner plexiform layer; OPL, outer plexiform layer; ONL, outer nuclear layer. Images courtesy of Ralph Eagle, MD.

However, patients with type 1 and 2 lesions harbored many similar features of AMN, including demographic risk factors, such as vasopressor exposure; presenting symptoms, such as paracentral scotoma; presenting clinical findings, such as paracentral macular lesions that were dark gray with NIR; and hyperreflective SD-OCT lesions that affected the OPL junction and could be explained by ischemia of the adjacent SCP (type 1) or DCP (type 2). It is more difficult to explain when a type 1 vs type 2 lesion will develop, but it is possible that younger patients may be more resistant to middle macular ischemia and may only be prone to watershed ischemic insults that affect the OPL/ONL region and the outer macula due to more severe vasculopathic injury. The consistent development of both type 1 and 2 lesions focally in the parafoveal region may be attributed to the greater density of the capillary network in this area.

Our suggested pathogenesis of focal retinal capillary ischemia would imply that AMN has little in common with any of the other acute zonal occult outer retinopathy complex disorders, one of the hypotheses proposed by Gass,<sup>22,27-29</sup> with which it has occasionally been grouped. Although the acute zonal occult outer retinopathy complex group includes conditions that are associated with IS/OS loss and subsequent reconstitution (eg, multiple evanescent white dot syndrome),<sup>30-32</sup>

it is clear from this case series and the one by Fawzi et al<sup>4</sup> that middle macular disease involving the OPL region as demonstrated by SD-OCT may be a prominent form of the disease. These characteristic middle macular lesions and the association with various ischemic causes serve to clearly distinguish AMN from the acute zonal occult outer retinopathy complex group of disorders that are more likely autoimmune or inflammatory mediated.

In summary, it appears that AMN is not nearly as rare a disorder as previously thought. The diagnosis of AMN has vastly improved with the use of multimodal imaging, including NIR imaging and SD-OCT. Two types of AMN lesions may be appreciated with SD-OCT analysis occurring above and below the OPL. Type 1 refers to hyperreflective bands in the OPL/INL region with subsequent INL thinning, which we describe as a paracentral acute middle maculopathy. Type 2 refers to hyperreflective bands in the OPL/ONL region with subsequent ONL thinning and outer macular disruption. We propose that each of these lesions may be explained by vasoconstriction or occlusion of the SCP (type 1) or DCP (type 2) located in the innermost and outermost portion of the INL, respectively, immediately adjacent to each corresponding lesion type.

#### ARTICLE INFORMATION

**Submitted for Publication:** December 24, 2012; final revision received February 2, 2013; accepted February 20, 2012.

**Published Online:** August 8, 2013.  
doi:10.1001/jamaophthalmol.2013.4056.

**Author Affiliations:** Jules Stein Eye Institute, University of California-Los Angeles (Sarraf, Rahimy, Beardsley); Greater Los Angeles Veterans Affairs Healthcare Center, Los Angeles, California (Sarraf, Rahimy); Department of Ophthalmology, Feinberg School of Medicine, Northwestern University, Chicago, Illinois (Fawzi); Department of Ophthalmology, University of Iowa Hospital, Iowa City (Sohn); Vitreous Retina Macula Consultants of New York, New York (Barbazetto, Klancnik, Mrejen,

Sorenson, Freund); Department of Ophthalmology, New York University School of Medicine, New York (Barbazetto, Klancnik, Mrejen, Sorenson, Freund); Kellogg Eye Center, University of Michigan, Ann Arbor (Zacks); VitreoRetinal Surgery, PA, Minneapolis, Minnesota (Mittra); Department of Ophthalmology, Mount Sinai School of Medicine, New York, New York (Goldberg).

**Author Contributions:** Drs Sarraf and Rahimy are co-first authors.

**Study concept and design:** Sarraf, Rahimy, Sohn, and Freund.

**Acquisition of data:** Sarraf, Rahimy, Fawzi, Sohn, Barbazetto, Zacks, Mittra, Klancnik, Mrejen, Goldberg, Beardsley, Sorenson, and Freund.

**Analysis and interpretation of data:** Sarraf, Rahimy,

Fawzi, Sohn, Barbazetto, Zacks, Mittra, Mrejen, and Freund.

**Drafting of the manuscript:** Sarraf, Rahimy, Sohn, Beardsley, and Freund.

**Critical revision of the manuscript for important intellectual content:** Sarraf, Rahimy, Fawzi, Sohn, Barbazetto, Mittra, Klancnik, Mrejen, Goldberg, Sorenson, and Freund.

**Statistical analysis:** Rahimy.

**Administrative, technical, and material support:** Sarraf, Rahimy, and Goldberg.

**Study supervision:** Sarraf, Fawzi, Sohn, Barbazetto, Mittra, and Freund.

**Patient examinations:** Beardsley.

**Conflict of Interest Disclosures:** None reported.

**Funding/Support:** This study was supported by the Karl Kirchgessner Foundation (Dr Sarraf) and Macula Foundation Inc (Dr Freund).

**Additional Information:** Drs Sarraf and Rahimy are both first authors for this article.

## REFERENCES

- Bos PJ, Deutman AF. Acute macular neuroretinopathy. *Am J Ophthalmol*. 1975;80(4):573-584.
- Yeh S, Hwang TS, Weleber RG, Watzke RC, Francis PJ. Acute macular outer retinopathy (AMOR): a reappraisal of acute macular neuroretinopathy using multimodality diagnostic testing. *Arch Ophthalmol*. 2011;129(3):365-368.
- Hughes EH, Siow YC, Hunyor AP. Acute macular neuroretinopathy: anatomic localisation of the lesion with high-resolution OCT. *Eye (Lond)*. 2009;23(11):2132-2134.
- Fawzi AA, Pappuru RR, Sarraf D, et al. Acute macular neuroretinopathy: long-term insights revealed by multimodal imaging. *Retina*. 2012;32(8):1500-1513.
- Lombardo M, Serrao S, Ducoli P, Lombardo G. Variations in image optical quality of the eye and the sampling limit of resolution of the cone mosaic with axial length in young adults. *J Cataract Refract Surg*. 2012;38(7):1147-1155.
- Lombardo M, Lombardo G, Ducoli P, Serrao S. Adaptive optics photoreceptor imaging. *Ophthalmology*. 2012;119(7):1498-1492.e2.
- Baumüller S, Holz FG. Early spectral-domain optical coherence tomography findings in acute macular neuroretinopathy. *Retina*. 2012;32(2):409-410.
- Neuhann IM, Inhoffen W, Koerner S, Bartz-Schmidt KU, Gelissen F. Visualization and follow-up of acute macular neuroretinopathy with the Spectralis HRA+OCT device. *Graefes Arch Clin Exp Ophthalmol*. 2010;248(7):1041-1044.
- Vance SK, Spaide RF, Freund KB, Wiznia R, Cooney MJ. Outer retinal abnormalities in acute macular neuroretinopathy. *Retina*. 2011;31(3):441-445.
- Monson BK, Greenberg PB, Greenberg E, Fujimoto JG, Srinivasan VJ, Duker JS. High-speed, ultra-high-resolution optical coherence tomography of acute macular neuroretinopathy. *Br J Ophthalmol*. 2007;91(1):119-120.
- Tan PE, Yu PK, Balaratnasingam C, et al. Quantitative confocal imaging of the retinal microvasculature in the human retina. *Invest Ophthalmol Vis Sci*. 2012;53(9):5728-5736.
- Lujan BJ, Roorda A, Knighton RW, Carroll J. Revealing Henle's fiber layer using spectral domain optical coherence tomography. *Invest Ophthalmol Vis Sci*. 2011;52(3):1486-1492.
- Birol G, Wang S, Budzynski E, Wangsa-Wirawan ND, Linsenmeier RA. Oxygen distribution and consumption in the macaque retina. *Am J Physiol Heart Circ Physiol*. 2007;293(3):H1696-H1704.
- Stone J, van Driel D, Valter K, Rees S, Provis J. The locations of mitochondria in mammalian photoreceptors: relation to retinal vasculature. *Brain Res*. 2008;1189:58-69.
- Wangsa-Wirawan ND, Linsenmeier RA. Retinal oxygen: fundamental and clinical aspects. *Arch Ophthalmol*. 2003;121(4):547-557.
- O'Brien DM, Farmer SG, Kalina RE, Leon JA. Acute macular neuroretinopathy following intravenous sympathomimetics. *Retina*. 1989;9(4):281-286.
- El-Dairi M, Bhatti MT, Vaphiades MS. A shot of adrenaline. *Surv Ophthalmol*. 2009;54(5):618-624.
- Desai UR, Sudhamathi K, Natarajan S. Intravenous epinephrine and acute macular neuroretinopathy. *Arch Ophthalmol*. 1993;111(8):1026-1027.
- Browning AC, Gupta R, Barber C, Lim CS, Amoaku WM. The multifocal electroretinogram in acute macular neuroretinopathy. *Arch Ophthalmol*. 2003;121(10):1506-1507.
- Lalezary M, Schoenberger SD, Cherney E, Agarwal A. Acute macular neuroretinopathy: an atypical case. *Retin Cases Brief Rep*. 2013;7(1):5-8.
- Kerrison JB, Pollock SC, Bioussé V, Newman NJ. Coffee and doughnut maculopathy: a cause of acute central ring scotomas. *Br J Ophthalmol*. 2000;84(2):158-164.
- Gass JD. *Stereoscopic Atlas of Macular Disease Diagnosis and Treatment*. St Louis, MO: CV Mosby Co; 1977.
- Turbeville SD, Cowan LD, Gass JD. Acute macular neuroretinopathy: a review of the literature. *Surv Ophthalmol*. 2003;48(1):1-11.
- Gillies M, Sarks J, Dunlop C, Mitchell P. Traumatic retinopathy resembling acute macular neuroretinopathy. *Aust N Z J Ophthalmol*. 1997;25(3):207-210.
- Leys M, Van Slycken S, Koller J, Van de Sompel W. Acute macular neuroretinopathy after shock. *Bull Soc Belge Ophthalmol*. 1991;241:95-104.
- Corver HD, Ruys J, Kestelyn-Stevens AM, De Laey JJ, Leroy BP. Two cases of acute macular neuroretinopathy. *Eye (Lond)*. 2007;21(9):1226-1229.
- Gass JD. Are acute zonal occult outer retinopathy and the white spot syndromes (AZOOR complex) specific autoimmune diseases? *Am J Ophthalmol*. 2003;135(3):380-381.
- Gass JD. Acute zonal occult outer retinopathy: Donders Lecture: The Netherlands Ophthalmological Society, Maastricht, Holland, June 19, 1992. *J Clin Neuroophthalmol*. 1993;13(2):79-97.
- Gass JD, Hamed LM. Acute macular neuroretinopathy and multiple evanescent white dot syndrome occurring in the same patients. *Arch Ophthalmol*. 1989;107(2):189-193.
- Spaide RF, Koizumi H, Freund KB. Photoreceptor outer segment abnormalities as a cause of blind spot enlargement in acute zonal occult outer retinopathy-complex diseases. *Am J Ophthalmol*. 2008;146(1):111-120.
- Nguyen MH, Witkin AJ, Reichel E, et al. Microstructural abnormalities in MEWDS demonstrated by ultrahigh resolution optical coherence tomography. *Retina*. 2007;27(4):414-418.
- Li D, Kishi S. Restored photoreceptor outer segment damage in multiple evanescent white dot syndrome. *Ophthalmology*. 2009;116(4):762-770.